Transition Met Chem (2015) 40:715–722
DOI 10.1007/s11243-015-9966-6

Synthesis and characterization of transition metal complexes of a hexadentate N_4O_2 donor Schiff base ligand: X-ray crystal structures of the copper(II) and zinc(II) complexes and their antibacterial properties

Hassan Keypour[1] · Amir Shooshtari[1] · Majid Rezaeivala[2] · Fariba Mohsenzadeh[3] · Hadi Amiri Rudbari[4]

Received: 14 May 2015 / Accepted: 17 July 2015 / Published online: 5 August 2015

Abstract A potentially hexadentate N_4O_2 Schiff base ligand, L, has been synthesized by condensation of an aromatic diamine with 2-pyridinecarbaldehyde. The complexes $[MLNO_3]NO_3$ (M=Cu, Ni, Cd or Zn) and $[MlCl_2]$ (M=Co or Mn) were synthesized by the reactions of L with metal salts in methanol. Both free L and its complexes were characterized by physicochemical and spectroscopic methods. In addition, the crystal structures of $[CuLNO_3]$-NO_3 and $[ZnLNO_3]NO_3$ have been determined by single-crystal X-ray diffraction. In both complexes, the ligand L is coordinated via pyridine and azomethine nitrogen atoms to give a distorted octahedral geometry. These complexes have antibacterial activities against three Gram-positive and three Gram-negative bacteria, which in most cases exceed those of tobramycin and tetracycline as standards.

Electronic supplementary material The online version of this article (doi:10.1007/s11243-015-9966-6) contains supplementary material, which is available to authorized users.

✉ Hassan Keypour
haskey1@yahoo.com

✉ Majid Rezaeivala
mrezaeivala@hut.ac.ir; mrezaeivala@gmail.com

[1] Faculty of Chemistry, Bu-Ali Sina University, Hamedan 65174, Iran

[2] Department of Chemical Engineering, Hamedan University of Technology, Hamedan 65155, Iran

[3] Laboratory of Plant Cell Biology, Department of Biology, Bu-Ali Sina University, Hamedan 65174, Iran

[4] Faculty of Chemistry, University of Isfahan, Isfahan 81746-73441, Iran

Introduction

The use of Schiff bases in biological or therapeutic applications as promising drug agents or biological probes and analytical tools has been reported by several researchers. In particular, the bioactivities of Schiff bases as antibacterial [1, 2], antiradical [3, 4], anticancer [5], antifungal [6] and antiviral agents [7, 8] have been reported. Schiff bases derived from aromatic amines and aromatic aldehydes have a wide variety of applications in mimicking biological materials and naturally occurring compounds [9, 10].

Recently, we and others have reported the synthesis, characterization and antibacterial studies of some new Schiff base complexes [11–16]. The present work describes the synthesis and characterization of a new hexadentate N_4O_2 donor Schiff base ligand L and some of its metal complexes, including spectroscopic and X-ray crystallographic studies. In addition, their in vitro antibacterial activities were tested against three Gram-positive and three Gram-negative human pathogenic bacteria. The results indicated that these compounds have stronger activities than the standard antibiotics against some bacterial strains.

Experimental

Materials and methods

2-(2-((2-Aminophenoxy)methyl)benzyloxy)benzenamine was synthesized according to the literature procedure [17]. Solvents, 2-pyridinecarbaldehyde and metal salts were purchased from Merck and used without further purification.

Infrared spectra were collected using KBr pellets on a BIO-RAD FTS-40A spectrophotometer (4000–400 cm^{-1}).

A Perkin-Elmer Lambda 45 (UV–Vis) spectrophotometer was used to record the electronic spectra. CHN analyses were obtained using a Perkin-Elmer, CHNS/O elemental analyzer model 2400 series 2. Conductance measurements were taken using a Hanna HI 8820 conductivity meter. ^{1}H and ^{13}C NMR spectra were recorded in DMSO-d_6 on a Bruker Avance 400 MHz spectrometer using $Si(CH_3)_4$ as internal standard.

X-ray crystallography

Green crystals of $[CuLNO_3]NO_3$ and yellow crystals of $[ZnLNO_3]NO_3$ were grown by slow diffusion of diethyl ether vapor into an acetonitrile solution of each. X-ray data were collected on a STOE IPDS-II diffractometer with graphite-monochromated Mo–Kα radiation. Cell constants and an orientation matrix for data collection were obtained by least-squares refinement of diffraction data. Data were collected at a temperature of 298(2) K in a series of ω scans in 1° oscillations and integrated using the Stoe X-AREA [18] software package. A numerical absorption correction was applied using the X-RED [19, 20] and X-SHAPE [19, 20] software. The data were corrected for Lorentz and polarization effects. The structures were solved by direct methods using SIR2004 [21]. The non-hydrogen atoms were refined anisotropically by full-matrix least-squares methods on F^2 using SHELXL [22]. All hydrogen atoms were added at ideal positions and constrained to ride on their parent atoms. Crystallographic data for the complexes are listed in Table 1. Selected bond distances and angles are summarized in Table 3.

Antimicrobial assays

Some microorganisms were obtained from Persian Type Culture Collection, Tehran, Iran, and others were locally isolated (LI).

The standard strains of the following microorganisms were used as test organisms:

Bacillus thuringiensis (PTCC 1358), *Bacillus subtilis* (ATCC 6051), *Staphylococcous saprophyticus* (ATCC 6633), *Pseudomonas fluorescens* (PTCC 1310), *Pectobacterium* Sp. (LI), *Klebsilla axytoca* (LI).

The organisms were subcultured in nutrient broth and nutrient agar (Oxiod Ltd.) for use in experiments, while diagnostic sensitivity test agar (DST) (Oxoid Ltd.) was used in antibiotic sensitivity testing.

For bioassays, suspensions of approximately 1.5×10^8 cells per mL in sterile normal saline were prepared as described in the literature [23]. The sensitivity testing was determined using the agar-gel diffusion method [24, 25]. In each disk, 20 µL of each chemical, containing 10 µg in DMSO, was loaded. The minimum inhibitory concentration (MIC) of each test compound was also determined using a twofold dilution method [26]. The isolated bacterial strains were first grown in nutrient broth for 18 h before use. The inoculum suspensions were standardized and then tested against the test compound, using 20 µL for each disk in DST medium. The plates were then incubated at 37.0 ± 0.5 °C for 24 h after which they were observed for zones of inhibition. The effects were compared with those of the standard antibiotics tobramycin and tetracycline at a concentration of 1 mg/mL [27]. The MIC was also determined by tube dilution techniques in Mueller–Hinton broth (Merck) according to the literature procedure [28]. The experiments were repeated at least three times for each organism, and the data are presented as the mean ± SE of 3–5 samples.

Synthesis of L

A solution of 2-(2-((2-aminophenoxy)methyl)benzyloxy)benzenamine (0.320 g, 1 mmol) in methanol (20 mL) was added dropwise to a stirred solution of 2-pyridinecarbaldehyde (0.214 g, 2 mmol) in methanol (30 mL) (Scheme 1). The mixture was stirred at room temperature for 12 h. The yellowish precipitate so obtained was filtered off, washed with cold methanol and dried in vacuo. Yield: (0.41 g, 80 %). M.p. 79 °C. Anal. Calc. for $C_{32}H_{26}N_4O_2$: C, 77.1; H, 5.3; N, 11.2 found: C, 77.0; H, 5.1; N, 11.4 %. IR (cm^{-1}, KBr): 1629 (*s*, *v*C=N). ^{1}H NMR (DMSO d_6, ppm) δ_H: 5.369 (*s*, 4H, Ar–CH_2); 6.655–8.167 (*m*, 20H, Ar–H); 8.542 (*s*, 2H, Ar–CH=N). ^{13}C NMR (DMSO d_6, ppm) δ_C: 69.7 (C_4, C'_4), 117.8, 122.1, 122.5, 122.8, 127.1, 128.8, 129.4, 129.5, 129.7, 138.5, 139.4, 142.4, 146.8 (aromatic rings), 151.2 (C_{11}, C'_{11}). UV–Vis [λ (nm), ε (M^{-1} cm^{-1})]: 269(40,430), 275(42,320), 347(9310).

Synthesis of $[CdLNO_3]NO_3$

A methanolic solution (25 mL) of $Cd(NO_3)_2.6H_2O$ (0.3445 g, 1 mmol) was added slowly to a warm solution of L (0.498 g, 1 mmol) in methanol (50 mL). The mixture was stirred under reflux for 12 h. The resultant yellow precipitate was filtered off, washed with diethyl ether and dried under vacuum. Yield: 0.56 g (76 %). M.p. 277 °C. Anal. Calc. for $C_{32}H_{26}CdN_6O_8$ (MW: 735.0): C, 52.3; H, 3.6; N, 11.4 found: C, 52.1; H, 3.7; N, 11.3 %. IR (cm^{-1}, KBr): 1636 (*s*, *v*C=N). ^{1}H NMR (DMSO d_6, ppm) δ_H: 4.955 (*s*, 2H, Ar–CH_2); 6.817–8.004 (*m*, 18H, Ar–H); 8.042, 8.173 (*s*, 2H, H_{16}); 8.491, 8.589 (*d*, 2H, Ar–CH=N).^{13}C NMR (DMSO d_6, ppm) δ_C: 73.3(C_4, C'_4), 118.8, 119.7, 123.2, 124.2, 130.2, 130.6, 131.7, 136.4, 140.1, 141.9, 151.6, 151.9 (aromatic rings), 162.6 (C_{11}, C'_{11}). UV–Vis [λ (nm), ε (M^{-1} cm^{-1})]: 267(23,360), 275(21,990), 346(8670). $\Lambda_m = 107.7$ cm^2 Ω^{-1} mol^{-1}.

Table 1 Crystal data and structure refinement for $[CuLNO_3]NO_3$ and $[ZnLNO_3]NO_3$ complexes

Empirical formula	$C_{32}H_{26}CuN_6O_8$	$C_{32}H_{26}N_6O_8Zn$
Identification code	m_c2c	m + c2c
Formula weight	686.13	687.96
Temperature (K)	298(2)	298(2)
Wavelength (Å)	0.71073	0.71073
Crystal system	Monoclinic	Monoclinic
Space group	C2/c	C2/c
Unit cell dimensions		
a (Å)	36.755(7)	36.457(7)
b (Å)	10.920(2)	10.965(2)
c (Å)	16.337(3)	16.522(3)
α (°)	90	90
β (°)	109.56(3)	109.63(3)
γ (°)	90	90
Volume (Å^3)	6179(2)	6221(2)
Z	8	8
Calculated density (Mg/m$^{-3)}$	1.475	1.469
Absorption coefficient (mm^{-1})	0.769	0.852
F(000)	2824	2832
θ range for data collection (°)	2.47–29.20	2.46–25.00
Limiting indices	$-14 \leq h \leq 50$, $-14 \leq k \leq 14$, $-22 \leq l \leq 21$	$-43 \leq h \leq 12$, $-13 \leq k \leq 12$, $-18 \leq l \leq 19$
Reflections collected/unique [$R_{(int)}$]	14,916/8316 [0.0600]	9749/5473 [0.0433]
Completeness to $\theta = 25.00$ (%)	99.3	99.8
Refinement method	Full-matrix least-squares on F^2	Full-matrix least-squares on F^2
Data/restraints/parameters	8316/0/435	5473/0/435
Goodness-of-fit on F^2	1.049	0.926
Final R indices [$I > 2$sigma(I)]	$R1 = 0.0370$, $wR2 = 0.0707$	$R1 = 0.0341$, $wR2 = 0.0713$
R indices (all data)	$R1 = 0.1827$, $wR2 = 0.0848$	$R1 = 0.0731$, $wR2 = 0.0765$
Largest diff. peak and hole (e Å^{-3})	0.313 and −0.590	0.274 and −0.384

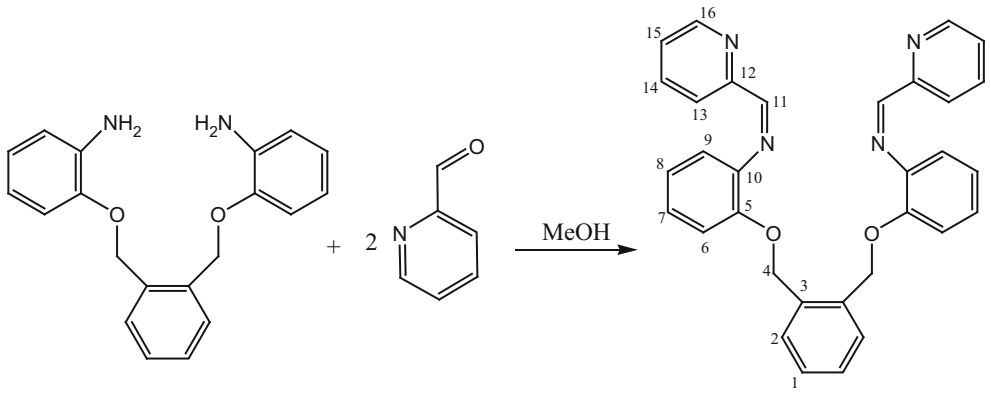

Scheme 1 Synthesis of macroacyclic Schiff base ligand (L) with NMR numbering

Synthesis of $[CuLNO_3]NO_3$

The preparation of this green microcrystalline complex followed the same procedure described for $[CdLNO_3]NO_3$, using a solution of $Cu(NO_3)_2{\cdot}6H_2O$ (0.2956 g, 1 mmol) in 25 mL of methanol. Yield: 0.49 g (71 %). M.p. 234 °C. Anal. Calc. for $C_{32}H_{26}CuN_6O_8$ (MW: 686.13): C, 56.0; H, 3.8; N, 12.2 found: C, 55.9; H, 3.9; N, 12.1 %. IR (cm^{-1},

KBr): 1632 (*s*, *v*C=N). UV–Vis [λ (nm), ε (M^{-1} cm^{-1})]: 267(14,760), 289(11,640), 348(7310), 508(244), 691(92). Λ_m = 144.4 cm^2 Ω^{-1} mol^{-1}.

Synthesis of $[CoLCl_2]H_2O$

The preparation of this red complex followed the same procedure described for $[CdLNO_3]NO_3$, by using a solution of $CoCl_2{\cdot}6H_2O$ (0.2378 g, 1 mmol) in 25 ml of methanol. Yield: 0.59 g (78 %). M.p. 346 °C. Anal. Calc. for $C_{32}H_{28}Cl_2CoN_4O_3$ (MW: 646.43): C, 59.5; H, 4.4; N, 8.7 found: C, 59.3; H, 4.5; N, 8.6 %. IR (cm^{-1}, KBr): 1642 (*s*, *v*C=N). UV–Vis [λ (nm), ε (M^{-1} cm^{-1})]: 268(44,470), 274(43,600), 344(9970), 545(1489), 680(208). Λ_m = 32.8 cm^2 Ω^{-1} mol^{-1}.

Synthesis of $[NiLNO_3]NO_3$

The preparation of this green complex followed the same procedure described for $[CdLNO_3]NO_3$, using a solution of $Ni(NO_3)_2{\cdot}6H_2O$ (0.2908 g, 1 mmol) in 25 mL of methanol. Yield: 0.53 g (78 %). M.p. 346 °C. Anal. Calc. for $C_{32}H_{26}NiN_6O_8$ (MW: 681.28): C, 56.4; H, 3.9; N, 12.3 found: C, 56.3; H, 4.0; N, 12.2 %. IR (cm^{-1}, KBr): 1645 (*s*, *v*C=N). UV–Vis [λ (nm), ε (M^{-1} cm^{-1})]: 266(35,570), 277(29,240), 335(4260), 493(210). Λ_m = 97.7 cm^2 Ω^{-1} mol^{-1}.

Synthesis of $[MnLCl_2]$

The preparation of this orange complex followed the same procedure described for $[CdLNO_3]NO_3$, using a solution of $MnCl_2{\cdot}4H_2O$ (0.1979 g, 1 mmol) in 25 mL of methanol. Yield: 0.49 g (78 %). M.p. 303 °C. Anal. Calc. for $C_{32}H_{26}Cl_2MnN_4O_2$ (MW: 624.42): C, 61.6; H, 4.2; N, 9.0 found: C, 61.4; H, 4.3; N, 8.8 %. IR (cm^{-1}, KBr): 1642 (*s*, *v*C=N). UV–Vis [λ (nm), ε (M^{-1} cm^{-1})]: 267(84,010), 276(85,560), 345(14,420), 490(233), 634(249). Λ_m = 24.4 cm^2 Ω^{-1} mol^{-1}.

Synthesis of $[ZnLNO_3]NO_3$

The preparation of this yellow microcrystalline followed the same procedure described for $[CdLNO_3]NO_3$, using a solution of $Zn(NO_3)_2{\cdot}6H_2O$ (0.2975 g, 1 mmol) in 25 mL of methanol. Yield: 0.56 g (82 %). M.p. 337 °C. Anal. Calc. for $C_{32}H_{26}ZnN_6O_8$ (MW: 687.97): C, 55.9; H, 3.8; N, 12.2 found: C, 55.7; H, 4.0; N, 12.1 %. IR (cm^{-1}, KBr): 167 (*s*, *v*C=N). ^{1}H NMR (DMSO d_6, ppm) δ_H: 4.957 (*s*, 4H, Ar–CH_2); 6.882–8.067 (*m*, 18H, Ar–H); 8.246, 8.337 (*s*, 2H, H_{16}); 8.668, 8.679 (*d*, 2H, Ar–CH=N). ^{13}C NMR (DMSO d_6, ppm) δ_C: 71.2 (C_4, C_4'), 117.8, 123.2, 125.0, 129.7, 130.1, 133.1, 136.8, 138.9, 143.1, 148.2, 150.6, 151.1 (aromatic rings), 163.1 (C_{11}, C_{11}'). UV–Vis [λ (nm), ε (M^{-1} cm^{-1})]: 269(27,268), 281(25,435), 314(9504). Λ_m = 108.3 cm^2 Ω^{-1} mol^{-1}.

Results and discussion

A new potentially hexadentate N_4O_2 Schiff base ligand L was readily prepared from the reaction between 2-(2-((2-aminophenoxy)methyl)benzyloxy)benzenamine and 2-pyridinecarbaldehyde. Complexes of L with copper(II), nickel(II), zinc(II) and cadmium(II) nitrate and also cobalt(II) and manganese(II) chloride were synthesized by template condensation reactions starting from the appropriate metal salt, 2-pyridinecarbaldehyde and 2-(2-((2-aminophenoxy) methyl)benzyloxy)benzenamine (mole ratio 1:1:1), respectively, in methanol. The same products were also obtained by direct condensation reactions of the metal salts with L in equimolar ratio in methanol. The composition of the products was not affected upon varying the mole ratio of reacting species. Molar conductivity measurements indicated that all the synthesized complexes except $[CoLCl_2]$ and $[MnLCl_2]H_2O$ are (1:1) electrolytes (see Experimental section). All of the complexes were characterized by elemental analysis, IR and UV–Vis. In addition, $[CdLNO_3]NO_3$ and $[ZnLNO_3]NO_3$ were characterized by ^{1}H and ^{13}C NMR spectroscopy and $[CuLNO_3]NO_3$ and $[ZnLNO_3]NO_3$ by X-ray diffraction (see "Experimental section" section, Tables 1, 3; Figs. 1, 2). The solid compounds are air stable and soluble in common organic solvents such as CH_3CN, $CHCl_3$, EtOH, MeOH and toluene.

Spectroscopic data

The IR spectra of these complexes show a sharp band in the range of 1632–1645 cm^{-1}, attributed to *v*(C=N), which is shifted to higher frequency compared with the free ligand (1629 cm^{-1} for L). Coordination of the imine nitrogen to the metal in these complexes is consistent with the X-ray diffraction results. The absence of C=O and N–H stretching vibrations in the spectra of free L and the complexes is consistent with Schiff base condensation. A band at 1384 cm^{-1} for $[CdLNO_3]NO_3$, $[CuLNO_3]NO_3$, $[NiLNO_3]NO_3$ and $[ZnLNO_3]NO_3$ is ascribed to the nitrate group stretching vibrations.

The electronic spectra of the free Schiff base and its metal complexes are summarized in Table 2. Free L shows three strong peaks at 269, 275 and 347 nm. The two strong bands at 269 and 275 nm are attributed to benzene $\pi \rightarrow \pi^*$ and imino $\pi \rightarrow \pi^*$ transitions, respectively [28]. The third band is assigned to $n \rightarrow \pi^*$ transitions. In the metal

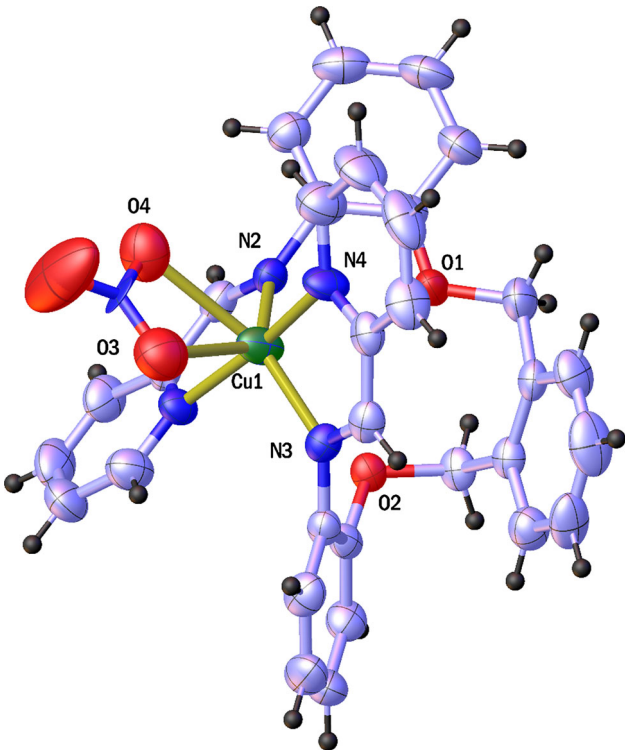

Fig. 1 ORTEP representation of $[CuLNO_3]NO_3$. Displacement ellipsoids are drawn at the 50 % probability level, and H atoms are shown as small spheres of arbitrary radii. The counter ion (nitrate) is omitted for clarity

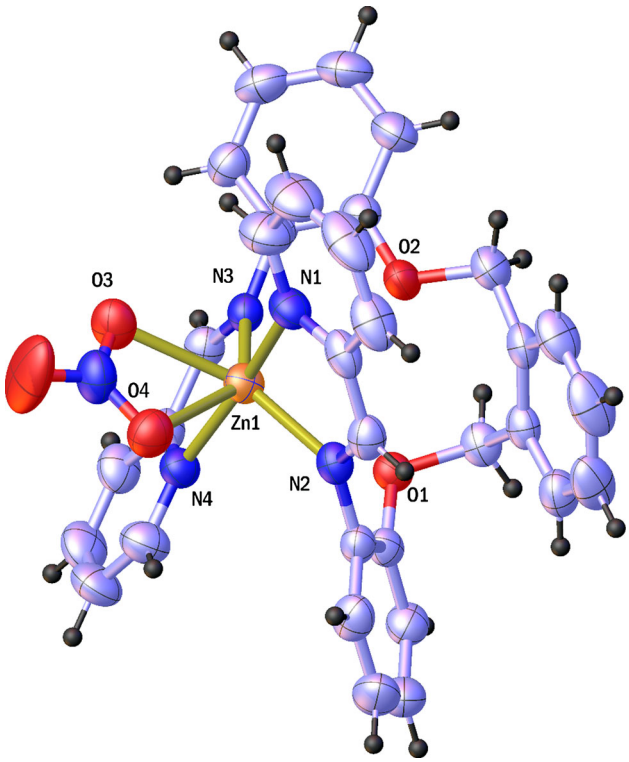

Fig. 2 ORTEP representation of $[ZnLNO_3]NO_3$. Displacement ellipsoids are drawn at the 50 % probability level, and H atoms are shown as small spheres of arbitrary radii. The counter ion (nitrate) is omitted for clarity

complexes, this band is shifted to shorter wavelengths. This shift may be attributed to the donation of the nitrogen atom lone pair of the Schiff base to the metal center (M ← N).

Electronic absorption spectra of the complexes were recorded in DMF solutions. Bands below 346 nm can be attributed to $\pi \rightarrow \pi^*$ and $n \rightarrow \pi^*$ transitions within the ligand. As can be seen in Table 2, in the electronic spectra of these complexes a charge transfer (CT) transition due to overlap with the $n \rightarrow \pi^*$ transition spectrum is not observed. The electronic spectrum of the Cu(II) complex displays a broad band at 691 nm assignable to the $^2Eg \rightarrow {}^2T_2g$ transition, characteristic of an octahedral geometry around Cu(II) [29]. The Ni(II) complex exhibited three bands at 550, 493 and 428 nm attributed to the $^3A_2g \rightarrow {}^3T_2g$ (ν_1), $^3A_2g \rightarrow {}^3T_1g(F)$ (ν_2) and $^3A_2g \rightarrow {}^3T_1g(P)$ (ν_3) transitions, respectively, indicating an octahedral geometry around the Ni(II) center [30]. The electronic spectrum of the Co(II) complex shows two absorption bands at 680 and 545 nm. These are assigned to the $^4T_1g(F) \rightarrow {}^4A_2g(F)$ and $^4T_1g(F) \rightarrow {}^4T_1g(P)$ transitions, respectively, characteristic of an octahedral geometry [31]. The complexes of Zn(II) and Cd(II) are diamagnetic without any *d–d* transitions. The Mn(II) complex also does not show any *d–d* transition [32].

Molar conductivities

The molar conductivity (Λ_M) data were measured at 25 °C using 10^{-3} M solutions of the complexes $[MLNO_3].NO_3$, (M=Ni, Cu, Cd or Zn) and $[MLCl_2]$, (M=Mn or Co) in DMF solution (see "Experimental" section). The results for the nitrate complexes suggest that one of the nitrate ions is coordinated directly to the central metal, while the other remains uncoordinated. The values for the chloride complexes indicate that both chlorides are coordinated to the metal. The elemental analyses are consistent with the proposed formulae, and that the ratio of M/L in all of these complexes is 1:1 [33, 34].

X-ray crystal structures

Suitable crystals of the copper(II) and zinc(II) complexes were obtained by slow diffusion of diethyl ether vapor into acetonitrile solutions of each complex. ORTEP views of these complexes are shown in Figs. 1 and 2, respectively. Crystallographic data and structure refinement parameters are given in Table 1, and selected bond distances and angles are given in Table 3.

Table 2 Electronic spectroscopy data (nm) for ligand (L) and related complexes

Compound[a]	λ_{max} (nm)(ε)[b]					
	Intraligand (LL)			*d–d*		
L	269(40,430)	275(42,320)	347(9310)			
$[MnLCl_2]$	267(84,010)	276(85,560)	345(14,420)			
$[CoLCl_2]$	268(44,470)	274(43,600)	344(9970)	545(1489)	680(208)	
$[NiLNO_3]NO_3$	266(35,570)	277(29,240)	335(4260)	428(615)[c]	493(210)	550(154)
$[CuLNO_3]NO_3$	267(14,760)	289(11,640)	346(7310)	691(92)		
$[CdLNO_3]NO_3$	267(23,360)	275(21,990)	346(8670)			
$[ZnLNO_3]NO_3$	269(27,268)	281(25,435)	344(9504)			

[a] All spectra were recorded in $CHCl_3$

[b] Mol^{-1} Cm^{-1}

[c] Shoulder

Both complexes display the same coordination geometry. In each complex, the ligand L coordinates to the metal center through the nitrogen atoms of the two pyridine rings [N(1) and N(4)] and the two nitrogen atoms of the imine groups [N(2) and N(3)], forming two five-membered chelate rings, while the etheric oxygen atoms [O(1)) and O(2)] remain uncoordinated. Furthermore, two oxygen atoms [O(3) and O(4)] of just one nitrate ligand form a four-membered chelate ring with the Cu(II) and Zn(II) centers, resulting in very distorted octahedral environments. As has been seen in similar cases [35, 36], this situation can be readily analyzed by examining the observed cis and trans angles {51.84(9)–135.65(10)° for $[CuLNO_3]NO_3$ and 55.65(8)–130.20(10)° for $[ZnLNO_3]NO_3$} and {134.79(11)–169.69(12)° for $[CuLNO_3]NO_3$ and 140.33(10)–168.46(10)° for $[ZnLNO_3]NO_3$}, respectively. The Cu(II) center in $[CuLNO_3]NO_3$ and Zn(II) center in $[ZnLNO_3]NO_3$ are both coordinated by N_4O_2 donor sets, such that the two pyridine nitrogen atoms [N(1) and N(4)] are disposed trans to each other with a bond angle of 169.69(12)° in the Cu complex and 168.46(10) in the Zn complex. Both oxygen atoms of the nitrate group [O(3) and O(4)] and two azomethine nitrogen atoms [N(2) and N(3)] occupy cis coordination sites with bond angles of 51.84(9)° and 135.65(10)° for $[CuLNO_3]NO_3$ and 55.65(8)° and 130.20(10)° for $[ZnLNO_3]NO_3$. The dihedral angle between the two five-membered chelate rings in $[CuLNO_3]NO_3$ (46.36(9)°) is significantly smaller than that in $[ZnLNO_3]NO_3$ (51.37(8)°).

As we have seen, the coordination mode of the nitrate groups, whether as monodentate or bidentate ligands, plays a crucial role in deviation from a regular octahedral structure [14].

Table 3 Selected bond lengths (Å) and bond angles (°) for complexes $[CuLNO_3]NO_3$ and $[ZnLNO_3]NO_3$

$[CuLNO_3]NO_3$		$[ZnLNO_3]NO_3$	
Bond	Distance	Bond	Distance
Cu(1)–N(1)	1.992(2)	Zn(1)–N(1)	2.135(2)
Cu(1)–N(2)	2.058(3)	Zn(1)–N(2)	2.069(3)
Cu(1)–N(3)	2.034(3)	Zn(1)–N(3)	2.065(2)
Cu(1)–N(4)	1.992(2)	Zn(1)–N(4)	2.146(2)
Cu(1)–O(3)	2.371(3)	Zn(1)–O(3)	2.299(3)
Cu(1)–O(4)	2.423(3)	Zn(1)–O(4)	2.309(3)
Bond	Angle	Bond	Angle
N(1)–Cu(1)–N(2)	81.19(11)	N(1)–Zn(1)–N(2)	79.07(10)
N(1)–Cu(1)–N(3)	100.57(11)	N(1)–Zn(1)–N(3)	109.75(10)
N(1)–Cu (1)–N(4)	169.69(12)	N(1)–Zn (1)–N(4)	168.46(10)
N(2)–Cu (1)–N(3)	135.65(10)	N(2)–Zn (1)–N(3)	130.20(10)
N(2)–Cu(1)–N(4)	104.94(11)	N(2)–Zn(1)–N(4)	100.82(10)
N(3)–Cu(1)–N(4)	80.97(12)	N(3)–Zn(1)–N(4)	79.29(10)
O(3)–Cu(1)–N(1)	86.94(11)	O(3)–Zn(1)–N(1)	86.16(10)
O(4)–Cu(1)–N(1)	84.87(10)	O(4)–Zn(1)–N(1)	83.37(10)
O(3)–Cu(1)–N(2)	134.79(11)	O(3)–Zn(1)–N(2)	142.57(9)
O(4)–Cu(1)–N(2)	83.60(10)	O(4)–Zn(1)–N(2)	88.36(10)
O(3)–Cu(1)–N(3)	89.34(11)	O(3)–Zn(1)–N(3)	87.14(9)
O(4)–Cu(1)–N(3)	140.72(10)	O(4)–Zn(1)–N(3)	140.33(10)
O(3)–Cu(1)–N(4)	82.87(11)	O(3)–Zn(1)–N(4)	87.18(9)
O(4)–Cu(1)–N(4)	87.57(11)	O(4)–Zn(1)–N(4)	85.09(9)
O(3)–Cu(1)–O(4)	51.84(9)	O(3)–Zn(1)–O(4)	55.65(8)

Antibacterial activities

Antibacterial activities of these compounds were studied against Gram-positive and Gram-negative bacterial strains (Table 4). All of the compounds inhibited the growth of bacterial strains, producing a zone of inhibition of diameter 6.0–25.0 mm. The most effective combinations were **1** against *Pectobacterium* Sp. and *Klebsiella oxytoca*, **2** against *Klebsiella oxytoca* and **5** against *B. thuringiensis*. In some cases, these compounds were even more effective than the standard antibiotics tobramycin and tetracycline.

Table 4 Antibacterial activity of the studied chemicals that was expressed as diameter of inhibition zone (mm) and minimum inhibitory concentration (MIC)

Microorganisms	Standards		Zone of inhibition (mm)					
			Main compounds					
	Tobramycin (10 mg mL^{-1})	Tetracyclin (30 mg mL^{-1})	$[MnLCl_2]$	$[CoLCl_2]$	$[NiLNO_3]NO_3$	$[CuLNO_3]NO_3$	$[ZnLNO_3]NO_3$	$[CdLNO_3]NO_3$
MIC (μg/mL)	4	8	12	2	12	16	8	4
Gram (−)								
P. fluorescens	5 ± 1	–	–	–	–	–	–	6 ± 1
Pectobacterium Sp.	4 ± 1	6 ± 1	–	25 ± 4	–	–	15 ± 2	10 ± 2
K. oxytoca	10 ± 2	–	11 ± 2	21 ± 3.2	14 ± 2	–	15 ± 3	18 ± 2
Gram (+)								
B. thuringiensis	6 ± 1	8 ± 1	12 ± 2	13 ± 1	15 ± 3	18 ± 3	12 ± 1	16 ± 3
S. saprophyticus	22 ± 4	15 ± 3	10 ± 2	14 ± 2	12 ± 2	11 ± 2	13 ± 1	13 ± 3
B. subtilis	13 ± 2	15 ± 2	–	–	–	–	–	–

Since comparison of the size of inhibition zones is generally not trustworthy, the MIC values of the compounds were also determined according to the previously reported method [39]. These test results indicated that the MIC values against the tested organisms varied between 2 against *Pectobacterium* Sp. to **16** against *B. thuringiensis* μg mL^{-1}. The standard antibiotic tobramycin showed MIC values 4 μg mL^{-1} and tetracycline 8 μg mL^{-1}. Hence, these compounds have stronger activities than the standard antibiotics against some bacterial strains.

Conclusion

In this paper, we have reported the synthesis and spectroscopic characterization of a series of complexes with a new Schiff base ligand derived from 2-(2-((2-aminophenoxy)methyl)benzyloxy)benzenamine. The X-ray crystal structures of $[CuLNO_3]NO_3$ and $[ZnLNO_3]NO_3$ show distorted octahedral geometries in which the Schiff base acts as a tetradentate ligand. The complexes have interesting antibacterial activities.

Acknowledgments We are grateful to the Faculty of Chemistry of Bu-Ali Sina University for financial supports.

References

1. Chaviara ATh, Cox PJ, Repana KH, Papi RM, Papazisis KT, Zambouli D, Kortsaris AH, Kyriakidis DA, Bolos CA (2004) J Inorg Biochem 98:1271–1283
2. Shankera K, Rohinia R, Ravindera V, Reddyb PM, Hob Y (2009) Spectrochim Acta Part A 73:205–211
3. Bala S, Uppal G, Kamboj S, Saini V, Prasad DN (2012) Med Chem Res 21:1–13
4. Wu H, Jia F, Kou F, Liu B, Yuan J, Bai Y (2011) Trans Met Chem 36:847–853
5. Wang M, Wang LF, Li YZ, Li QX, Xu ZD, Qu DM (2001) Trans Met Chem 26:307–310
6. Guo Z, Xing R, Liu S, Zhong Z, Ji X, Wang L, Li P (2007) Carbohydr Res 342:1329–1332
7. Jarrahpour A, Khalili D, De Clercq E, Salmi C, Brunel JM (2007) Molecules 12:1720–1730
8. Sriram D, Yogeeswari P, Myneedu NS, Saraswat V (2006) Bioorg Med Chem Lett 16:2127–2129
9. Metzler CM, Cahill A, Metzler DE (1980) J Am Chem Soc 102:6075–6082
10. Dudek GO, Dudek EP (1965) Chem Commun 19:464–466
11. Keypour H, Shayesteh M, Sharifi-Rad A, Salehzadeh S, Khavasi H, Valencia L (2008) J Organomet Chem 693:3179–3187
12. Keypour H, Shayesteh M, Golbedaghi R, Chehregani A, Blackman AG (2012) J Coord Chem 65:1004–1016
13. Keypour H, Shayesteh M, Rezaeivala M, Chalabian F, Valencia L (2013) Spectrochim Acta A 101:59–66
14. Keypour H, Shayesteh M, Rezaeivala M, Chalabian F, Elerman Y, Buyukgungor O (2013) J Mol Struct 1032:62–68

15. Keypour H, Shooshtari A, Rezaeivala M, Kup FO, Rudbari HA (2015) Polyhedron 97:75–82
16. Sahin D, Hayvali Z (2012) J Incl Phenom Macro Chem 72:289–297
17. Fenton DE, Mattews RW, McPartlin M, Murphy BP, Scowen IJ, Tasker PA (1996) Dalton Trans 16:3421–3427
18. X-AREA (2005) Version 1.30, program for the acquisition and analysis of data. Stoe & Cie GmbH, Darmstadt
19. X-RED (2005) Version 1.28b, program for data reduction and absorption correction. Stoe & Cie GmbH, Darmstadt
20. X-SHAPE (2004) Version 2.05, program for crystal optimization for numerical absorption correction. Stoe & Cie GmbH, Darmstadt
21. Burla MC, Caliandro R, Camalli M, Carrozzini B, Cascarano GL, De Caro L, Giacovazzo C, Polidori G, Spagna R (2005) J Appl Crystallogr 38:381–388
22. Sheldrick GM (2008) Acta Crystallogr A 64:112–122
23. Forbes BA, Sahm DF, Weissfeld AS, Trevino EA (1990) Methods for testing antimicrobial effectiveness. In: Baron EJ, Peterson LR, Finegold SM (eds) Bailey & Scott's diagnostic microbiology, 8th ed. Mosby Co, St Louis, pp 171–194
24. Russel AD, Furr JR (1977) J Appl Bacteriol 43:23–25
25. Chehregani A, Mohsenzadeh F, Mirazi N, Hajisadeghian S, Baghali S (2010) Pharm Biol 48:1280–1284
26. Performance standards for antimicrobial susceptibility testing; Ninth informational supplement (2008) NCCLS document M100-S9. National Committee for Clinical Laboratory Standards, Wayne
27. Khan MR, Omosto AD (2003) Fitoterapia 74:4494–4497
28. Dyke SF, Floyd AJ, Sainsbury M, Theobald RS (1978) Organic spectroscopy—an introduction. Longman, New York
29. Liu H, Wang H, Gao F, Niu D, Lu Z (2007) J Coord Chem 60:2671–2678
30. Patil SA, Unki SN, Kulkarni AD, Naik VH, Badami PS (2011) Spectrochim Acta A 79:1128–1136
31. Anan NA, Hassan SM, Saad EM, Butler IS, Mostafa SI (2011) Carbohydr Res 346:775–793
32. Banerjee S, Ray A, Sen S, Mitra S, Hughes DL, Butcher RJ, Batten SR, Turner DR (2008) Inorg Chim Acta 361:2692–2700
33. Abou-Hussein AA, Linert W (2015) Spectrochim Acta A 141:223–232
34. Montazerozohori M, Khani S, Tavakol H, Hojjati A, Kazemi M (2011) Spectrochim Acta Part A 81:122–127
35. Khandar AA, Cardin C, Hosseini-Yazdi SA, McGrady J, Abedi M, Zarei SA, Gan Y (2010) Inorg Chim Acta 363:4080–4087
36. Khandar AA, White J, Taghvaee-Yazdeli T, Hosseini-Yazdi SA, McArdle P (2013) Inorg Chim Acta 400:203–209